

Equilibrium, kinetics and thermodynamics of biosorption of U(VI) by *Jonesia quinghaiensis* strain ZFSY-01 isolated from the wastewater of a uranium mine

Gen Xie, Henglei Chen, Peihong Mao and Guangwen Feng*

Research Center of Radiation Ecology and Ion Beam Biotechnology, College of Physics Science and Technology, Xinjiang University, Urumqi, Xinjiang 830017, China

*Corresponding author. E-mail: feng_guang_wen@163.com

ABSTRACT

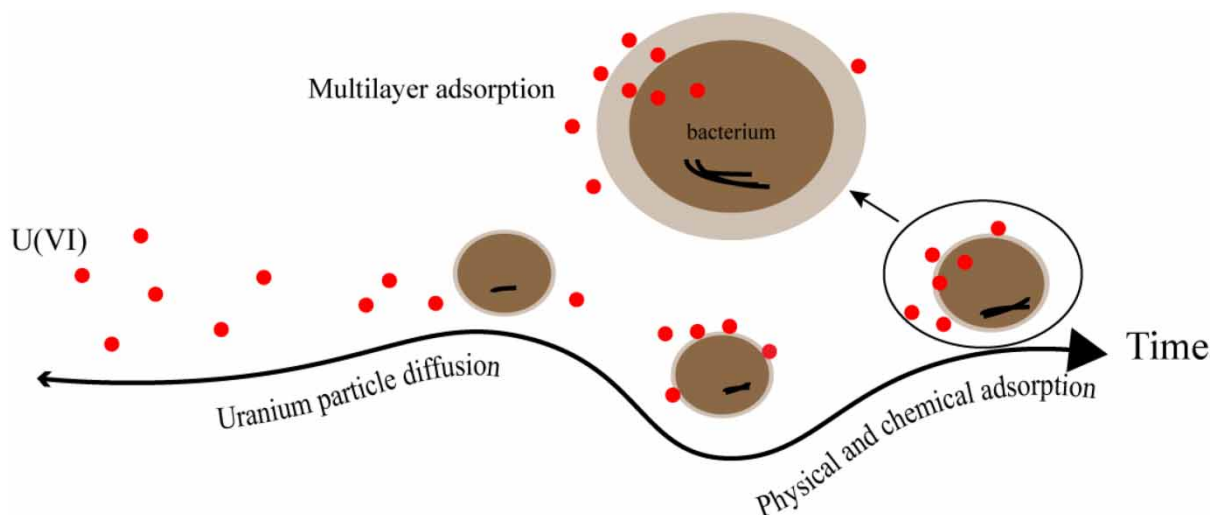
The adsorption ability of a native *Jonesia quinghaiensis* strain ZFSY-01, a microorganism isolated from uranium tailing wastewater, to U(VI) in wastewater under different conditions was studied in this work. The results showed that 391.5 mg U/g and 78.3% of adsorption capacity and efficiency were achieved under an optimum adsorption condition, respectively. Especially, the adsorption capacity of this strain reached the maximum ($Q=788.9$ mg U/g) under 100 mg/L of strain dosage. Simultaneously, the linear regression coefficients for the used isothermal sorption model indicate that the biosorption process is compatible with the Freundlich isotherm, the Temkin isotherm and the Halsey isotherm model. Based on the fitted kinetic parameters, the data from the experiments fit well with models of pseudo-second-order kinetics and intra-particle diffusion, suggesting that the strain ZFSY-01 immobilized U(VI) by physical and chemical adsorption. In addition, thermodynamic parameters demonstrated that the sequestration of U(VI) by the strain is spontaneous and endothermic. Based on the above analysis, strain ZFSY-01 can effectively remove U(VI) ions from high- or low-concentration uranium-containing wastewater and is expected to become a promising biological adsorbent.

Key words: biosorption, isothermal, kinetic, uranium-containing wastewater

HIGHLIGHTS

- Specific microbes in special habitats have potential efficacy.
- Adsorption capacity of strain ZFSY-01 reached 788.9 mg U/g under 100 mg/L of dosage.
- Strain ZFSY-01 immobilized U(VI) by physical and chemical adsorption.
- It is expected to be a green and efficient biosorbent material.

GRAPHICAL ABSTRACT



This is an Open Access article distributed under the terms of the Creative Commons Attribution Licence (CC BY-NC-ND 4.0), which permits copying and redistribution for non-commercial purposes with no derivatives, provided the original work is properly cited (<http://creativecommons.org/licenses/by-nc-nd/4.0/>).

1. INTRODUCTION

The increasing application of nuclear energy has resulted in the emission of large quantities of radioactive wastes containing uranium (U) (Banala *et al.* 2021a; Banerjee *et al.* 2022). Among these radioactive wastes, U is mainly present as U(IV) and U(VI) in two fugitive forms, where U(IV) exists as insoluble sediment and U(VI) is mainly in the form of uranyl (UO_2^{2+}), with higher radiological and chemical toxicity (Maolin *et al.* 2022; Sourav *et al.* 2022). It should be noted that uranium is a radioactive heavy metal; small amounts of uranium ingested by plants and animals will destroy the genetic information of cells leading to reproductive disorders, while excessive input of uranium can cause organ failure and even death in the human body (Song *et al.* 2019; Banala *et al.* 2021a). If the wastewater is unreasonably remediated, the uranium ions in the wastewater may infiltrate into the soil and groundwater, causing serious ecological contamination as well as eventually affecting people's health by means of the food chain (Nie *et al.* 2022). Therefore, the treatment of uranium-containing wastewater is an issue of concern.

Nowadays, the commonly used treatment methods for uranium-containing wastewater include chemical sedimentation, redox, ion exchange and adsorption (Gupta *et al.* 2018; Pudza & Abidin 2020). However, these traditional physicochemical approaches have their own limitations, such as higher costs, generation of secondary pollutants as well as cumbersome treatment processes, which do not conform to the goals of sustainable development (Lakaniemi *et al.* 2019; Silas *et al.* 2022). Whereas the bioremediation method just meets this demand. Compared with traditional methods, it has the advantages of low material cost, high adsorption efficiency and excellent selectivity. It is well known that, among all wastewater bioremediation technologies, microbial adsorption is considered a promising yet environmentally friendly way of recovering uranium or other heavy metals (Yu *et al.* 2021; Sivashankar *et al.* 2022; Smjecanin *et al.* 2022).

According to previous reports, bacteria have been found to have an excellent binding capacity for metallic uranium ions as a biosorbent. For example, the *Kocuria* sp. strain studied by Wang *et al.* immobilized U(VI) with a biosorption capacity of 104 mg U/g through phosphate on the bacterial surface (Wang *et al.* 2018). Subsequently, Sánchez-Castro *et al.* studied a strain of *Stenotrophomonas* Br8 with an adsorption capacity of 373 mg U/g, which showed high phosphatase activity (Sánchez-Castro *et al.* 2020), and Yu *et al.* isolated the *Pseudomonas stutzeri* strain with an adsorption capacity of 308.72 mg U/g from seawater that is expected to be an adsorbent material for the extraction of uranium from seawater (Yu *et al.* 2022). Some of them can immobilize heavy metals using the diversity and abundance of functional groups on the cell surface, or accumulate heavy metals in the cell utilizing cellular metabolism (Beni & Esmaeili 2020). However, due to the structural and functional variability of different microorganisms, their ability to bind and tolerance to uranium varies. Moreover, a large amount of literature showed that indigenous microorganisms isolated from uranium-contaminated areas have a high tolerance to the heavy metal uranium and other toxic substances (Islam & Sar 2011; Banala *et al.* 2021b). Based on the foregoing description, it seems of interest to study indigenous strains isolated from uranium contamination. In this work, a strain was isolated from a uranium mine in north-western China using a screening medium with different uranium concentrations (100, 300, and 500 mg/L) that showed a high tolerance to uranium, named ZFSY-01. The strain was identified as *Jonesia quinghaiensis* based on the 16S rRNA gene sequence (GenBank Accession No. NR029030.1). To our knowledge, there are no reported studies on the immobilization of uranium for *J. quinghaiensis* strain ZFSY-01. Thus, the primary purpose of the study was to investigate the removal ability of *J. quinghaiensis* strain ZFSY-01 to UO_2^{2+} in wastewater. First, the effects of different adsorption conditions (such as reaction time, temperature, strain dosage, system initial pH, and initial uranium concentration) on the adsorption performance of strain ZFSY-01 were studied to determine the optimal adsorption conditions. Secondly, the experimental data of uranium ion adsorption by strain ZFSY-01 were analyzed using various biosorption kinetics, thermodynamics as well as adsorption equilibrium models, and the fitting effects of various models were compared. Finally, the adsorption mechanism of uranium ion by strain ZFSY-01 was preliminarily explored.

2. MATERIALS AND METHODS

2.1. Experimental reagents

In this study, Luria Broth (LB) medium was used to culture the strain, in which tryptone and yeast extract were procured from Qingyao Bioengineering Co., Ltd (Qingdao, China), while sodium chloride (NaCl) was provided by Chengdu Kelong Chemical Co., Ltd (Chengdu, China). All experimental chemical substances were of analytical grade and did not need to be purified, and the solutions were prepared with sterile deionized water. Moreover, the uranium solvent used in the experiments was

obtained by diluting uranyl nitrate standard stock solution (1,000 mg/L), which was purchased from ANPEL Scientific Instrument Co., Ltd (Shanghai, China).

2.2. Source and collection of experimental strain ZFSY-01

The strain ZFSY-01 was isolated from an evaporation pond of a uranium mine waste stream in Northwest China and cultured using an LB medium, as detailed in the Supplementary Information. In order to obtain a single colony, the target strain was purified several times through serial culture and then identified by 16S rRNA gene sequencing. The specific molecular biological identification of strain ZFSY-01 was completed by Sangon Biotech (Shanghai) Co., Ltd. In addition, the strain ZFSY-01 was incubated in a medium at 30 °C with shaking of 180 rpm for 12 h and further collected for subsequent experiments. The bacterial cells were collected by centrifugation at 6,000 rpm for 10 min at 4 °C and washed 2–3 times with sterile water.

2.3. Uranium tolerance of strain ZFSY-01

The tolerance of the strain ZFSY-01 for uranium was determined. The bacteria were inoculated in an LB liquid medium with a uranium concentration gradient of 0, 50, 100, 200 and 300 mg/L and incubated with shaking (30 °C, 180 rpm). Then, samples were collected at 0, 2, 4, 6, 8, 14, 24, 36 and 48 h intervals to determine the optical density (OD) values and plot the growth curves of the strains so that the effect of different uranium concentrations on the growth of the strains could be studied. The species distribution of uranium was modeled by Visual MINTEQ version 3.0 at 200 mg/L of initial uranium concentration and $T = 30$ °C between pH 2 and 10.

2.4. Experiments on the immobilization of U(VI) by strain ZFSY-01 under different factors

A batch experimental method was used in this work to evaluate the adsorption properties of strain ZFSY-01 for U(VI) in solution. Under laboratory conditions, the effects of reaction time, temperature, strain dosage, system initial pH and initial uranium concentration on the immobilization of uranium by the strain were investigated sequentially. First, wet strain cells of 20 mg of dry weight were added to 50 ml of uranium-containing an LB liquid medium with a uranium concentration of 200 mg/L and incubated in a constant temperature oscillating incubator (30 °C, 180 rpm). Subsequently, the samples were removed and centrifuged at defined time intervals to separate the supernatant, in which U(VI) concentration was determined using the uranium estimation method (Arsenazo-III) (Banala *et al.* 2021a). Without adding biomass as a control group, the influence of container wall and LB medium on uranium sorption was eliminated.

The adsorption efficiency $R(\%)$ and adsorption capacity Q (mg/g) of uranium by bacteria were computed by Equations (1) and (2) (Silas *et al.* 2022):

$$R(\%) = (C_0 - C_e) / C_0 * 100\% \quad (1)$$

$$Q = (C_0 - C_e) * V / m \quad (2)$$

where C_0 and C_e were the initial and equilibrium concentrations of the uranium solution (mg/L), respectively. V is the volume of the liquid (ml) and m is the dry weight of the strain (g).

2.5. Experimental data analysis

All experiments were performed in triplicate, the experimental data were statistically analyzed using Microsoft Excel 2019, and the data were graphically plotted using Origin Pro 2021 software.

3. RESULT AND DISCUSSIONS

3.1. Uranium tolerance of strain ZFCW-01

The growth of the strain ZFSY-01 was largely unaffected by the heavy metal uranium compared to the control at a uranium concentration of 50 mg/L, as shown in Figure 1. Nevertheless, as the uranium concentration increased, it was noted that the growth of the strain decreased slightly in the same time period, which could be attributed to the chemical toxicity of uranium at high concentrations that inhibited the growth and metabolism of the strain. Overall, the strains maintained good cellular activity even at 300 mg/L of uranium concentration. Thus, it can be assumed that the strain has a high tolerance to uranium.

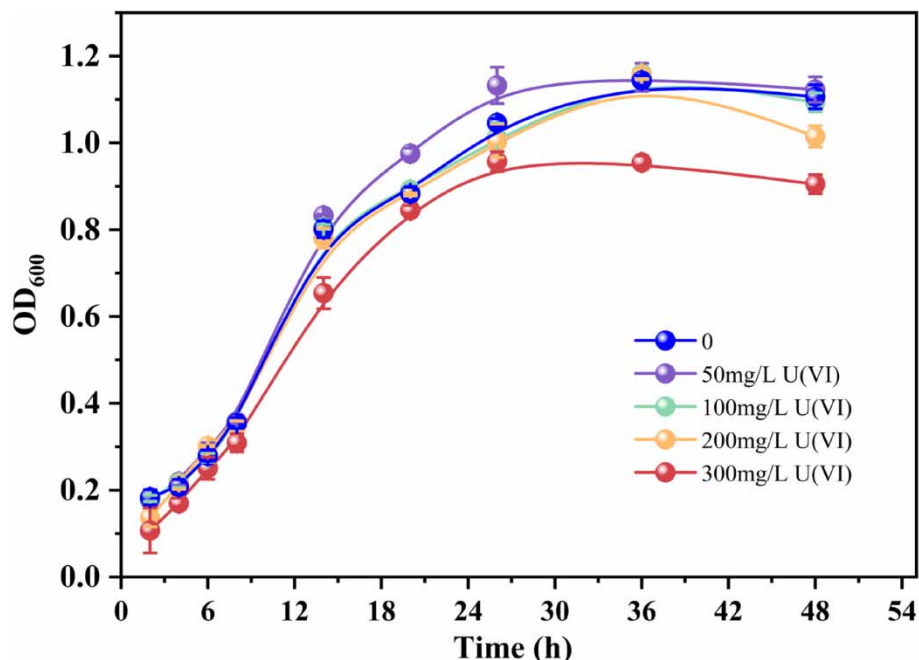


Figure 1 | The growth curve of strain ZFSY-01 at different uranium concentrations.

3.2. Effect analysis for experimental factors on the immobilized U(VI) of strain ZFSY-01

3.2.1. Reaction time

The influence of different reaction times on the uptake of U(VI) from strain ZFSY-01 was investigated. As shown in Figure 2(a), within 20–60 min, the adsorption efficiency of bacteria for U(VI) increased rapidly, reaching 55.49%. It is possible that the uranium ions in the solution bind rapidly to the active sites indicated by the bacteria at the initial stage, resulting in a rapid increase in adsorption efficiency. Between 60 and 200 min, the adsorption efficiency of U(VI) by bacteria only increased slowly. In the range of 200–240 min, when the adsorption capacity of bacteria was 314.75 mg U/g (Q_{max}), the adsorption efficiency of the bacteria was basically unchanged, which could be considered to be in a dynamic adsorption equilibrium. From the above analysis, it could be concluded that the optimal equilibration time for U(VI) adsorption by strain ZFSY-01 was 4 h, which was used for subsequent adsorption studies.

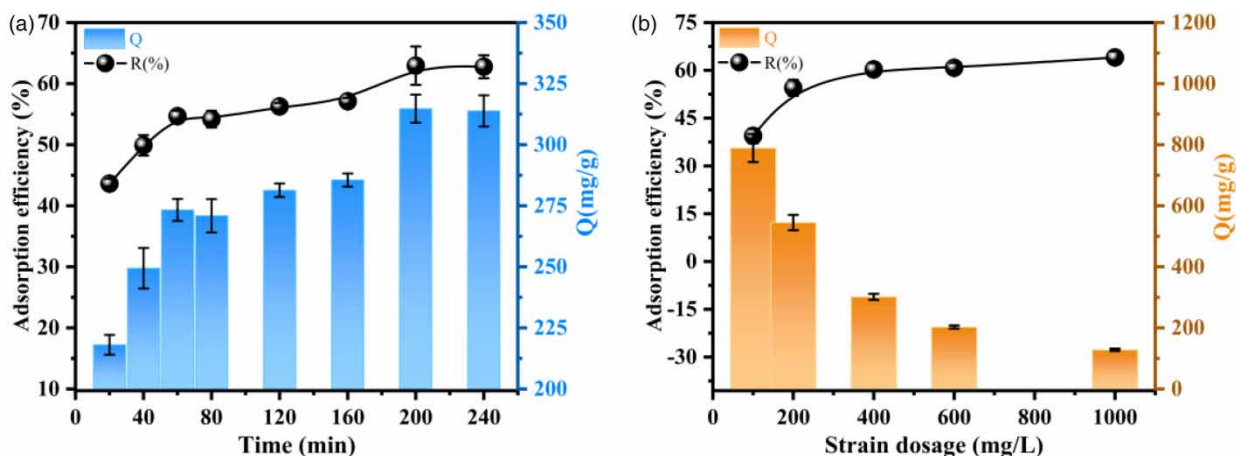


Figure 2 | (a) Effect of reaction time on U(VI) adsorption capacity and adsorption efficiency of strain ZFSY-01 (initial uranium concentration: 200 mg/L, V: 50 ml, T: 30 °C, strain dosage: 400 mg/L, pH: 6.5). (b) Effect of strain dosage on U(VI) adsorption capacity and adsorption efficiency of strain ZFSY-01 (initial uranium concentration: 200 mg/L, V: 50 ml, T: 30 °C, reaction time: 4 h, pH: 6.5).

3.2.2. Strain dosage

The dosage of the strain affects the efficiency of the adsorbent used, so it is very important to explore the optimal dosage of bacteria. In this study, the effect of different bacterial biomass on U(VI) adsorption was investigated in order to determine the optimal solid–liquid ratio for U(VI) adsorption by strain ZFSY-01, as indicated in Figure 2(b). Different concentrations of bacterial biomass were added to the LB liquid medium with an initial U(VI) concentration of 200 mg/L. The concentration range of added bacterial biomass was 100–1,000 mg/L (dry weight). As could be seen from Figure 1(b), with the increase in the dosage of bacteria, the adsorption efficiency of bacteria for uranium in LB liquid medium increased, while the adsorption capacity was the opposite. That is, the adsorption capacity of bacteria reached the maximum ($Q = 788.9$ mg/g) when the number of bacteria was 100 mg/L. Compared with other reported strains such as *Chryseomonas* MGF-48 (198 mg/g) (Malekzadeh *et al.* 2002), *Streptomyces levoris* (9.04 mg/g) (Tsuruta 2004), *Geobacillus thermoleovorans* subsp. (11 mg/g) (Özdemir & Kilinc 2012), *Bacillus thuringiensis* ZYR3 (355 mg/g) (Pan *et al.* 2015), *Bacillus subtilis* (alginate–chitosan microcapsules) (376.64 mg/g) (Tong 2017), *Bacillus amyloliquefaciens* (179.5 mg/g) (Liu *et al.* 2019) and *Candida albicans* (41.15 mg/g) (Liu *et al.* 2021), strain ZFSY-01 showed significantly higher adsorption capacity. When the dosage of the bacteria reached 400 mg/L, the adsorption efficiency of uranium by the strain increased to 60.3%, and the adsorption capacity of bacteria decreased to 312.49 mg U/g. After that, with the increase in the dosage of bacteria, the adsorption efficiency gradually tended to stabilize, reaching a maximum of 64.1%. This might be due to a ‘shielding’ influence on the cell face, which shielded the usable binding sites, thus reducing the ability of the strain to immobilize uranium (Malkoc & Nuhoglu 2005; Wang *et al.* 2010). Therefore, the optimal dosage of strain ZFSY-01 was considered to be 400 mg/L, considering the best adsorption efficiency of the bacteria on U(VI).

3.2.3. Initial pH

The pH of the solution plays an essential role in the adsorption process of uranium by microorganisms. This is because pH affects the main properties related to adsorption, such as the surface charge of the adsorption material, the degree of ionization and the species of metal ion binding states (Yu *et al.* 2016). As shown in Figure 3(a), the effect of strain ZFSY-01 on U(VI) removal in the LB liquid medium with different pH values was studied. As the pH increased from 3.0 to 5.0, the adsorption capacity and adsorption efficiency of strain ZFSY-01 for U(VI) increased with the increase of pH, which could be attributed to the high concentration of H^+ in LB medium under strongly acidic conditions, which competed with UO_2^{2+} . However, with the increase of pH in the solution, the H^+ ions in the solution decreased, with the result that UO_2^{2+} could be more involved in binding to the negatively charged active sites on the bacteria surface, thus raising the adsorption capacity of strain ZFSY-01 for U(VI) (Hu *et al.* 2018). Meanwhile, at pH 5.0, the maximum adsorption efficiency and the adsorption capacity of strain ZFSY-01 for U(VI) was observed simultaneously, i.e., the maximum adsorption efficiency was 78.3%, and the Q_{max} was 391.5 mg U/g, indicating that strain ZFSY-01 had the best adsorption efficiency for U(VI) in LB liquid medium solution at pH

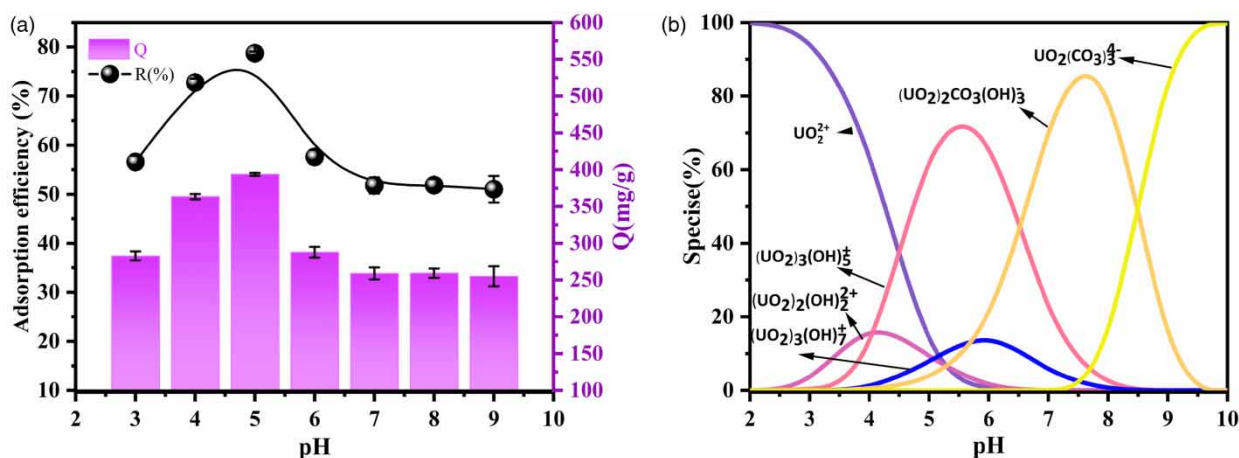


Figure 3 | (a) Effect of pH on U(VI) adsorption capacity and adsorption efficiency of strain ZFSY-01 (initial uranium concentration: 200 mg/L, V: 50 ml, T: 30 °C, strain dosage: 400 mg/L, reaction time: 4 h). (b) The species of uranium at different pH conditions was simulated with Visual MINEQL 3.0 (initial uranium concentration: 200 mg/L, T: 30 °C).

5.0. Notably, the adsorption capacity and the adsorption efficiency of uranium by bacteria showed a rapid decrease with increasing pH values between 5.0 and 9.0, and then began to stabilize. This could be explained by the increase of negatively charged uranium ions in solution with $\text{pH} > 5$, which repelled negatively charged active sites on the bacterial surface and inhibited the adsorption of U(VI) by bacterial cells (Salome *et al.* 2017; Li *et al.* 2019). In addition, Visual MINTEQ 3.0 software was applied to calculate the distribution of U(VI) species in solution at different pH conditions and the detailed results are reported in Table S2 of the Supplementary Information. The chemical speciation of uranium predicted under experimental conditions is shown in Figure 3(b), the pH of the solution was between 3.0 and 6.0, and the species of U(VI) in the solution were primarily present as UO_2^{2+} , $(\text{UO}_2)_3(\text{OH})_5^+$ and $(\text{UO}_2)_3(\text{OH})_7^+$ ions. Whereas the negatively charged uranium ions in solution, such as $\text{UO}_2(\text{CO}_3)(\text{OH})_3^-$ and $\text{UO}_2(\text{CO}_3)_3^{4-}$, mainly appeared at $\text{pH} > 7$ and gradually became prevalent (Ding *et al.* 2014).

3.2.4. Initial uranium concentration

Figure 4 shows the influence of adding different initial uranium concentrations (50–500 mg/L) on the adsorption of uranium by strain ZFSY-01 in the LB liquid medium. As the initial concentration of uranium added to the solution increased, the adsorption efficiency of the strain gradually decreased, while the adsorption capacity of uranium by the strain gradually increased and then tended to stabilize, that is, at an initial uranium concentration of 50 mg/L, the adsorption efficiency could reach 93.2%. When the concentration of initial uranium was above 300 mg/L, the uranium adsorption capacity was around 384.1 mg U/g and then tended to remain constant. This finding is in common with the results of Li *et al.* and Banala *et al.* for strains *Bacillus* sp. dwc-2 and *Bacillus aryabhattai* B8W22 (Li *et al.* 2014; Banala *et al.* 2021b). The reason for this phenomenon was that under certain bacterial dosage conditions, the number of active adsorption sites on the bacterial surface was determined. When the concentration of added uranium was low, most of the uranium in the solution could bind to the active sites. As the concentration of uranium increased, the active adsorption sites on the surface of bacteria that bind to uranium tended to become saturated, leaving excess uranium in a free state. Therefore, the finding indicated that the higher the initial uranium concentration, the lower the adsorption efficiency of bacteria for uranium, while the opposite is true for the adsorption capacity of bacteria for uranium.

3.3. Biosorption equilibrium analysis of uranium adsorption by strain ZFSY-01

To search the adsorption mechanism of U(VI) by strain ZFSY-01, the experimental data were fitted using Langmuir, Freundlich, Temkin, and Halsey adsorption isotherm models. The linear formula for Langmuir isotherm, Freundlich isotherm,

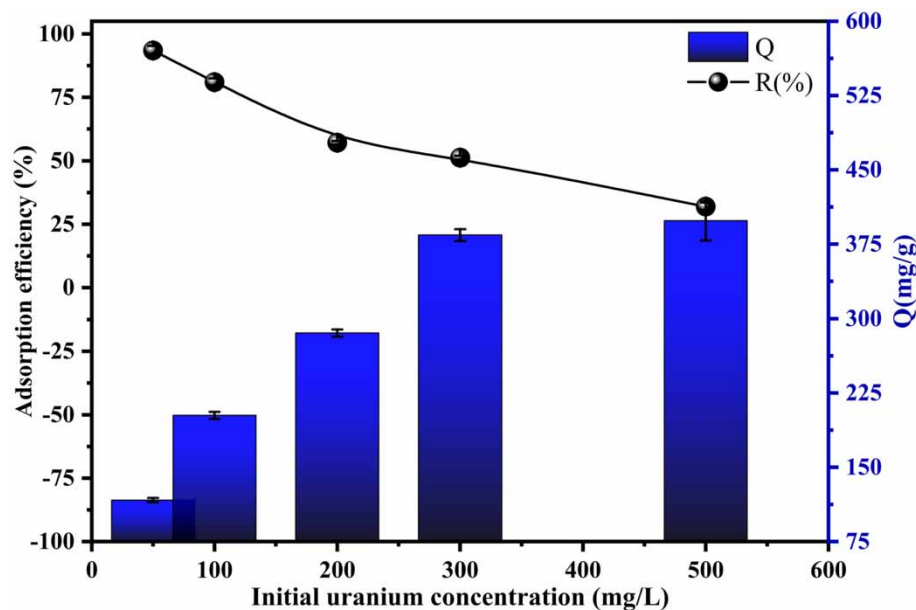


Figure 4 | Effect of initial uranium concentration on U(VI) adsorption capacity and adsorption efficiency of strain ZFSY-01 (V: 50 ml, T: 30 °C, strain dosage: 400 mg/L, reaction time: 4 h, pH: 6.5).

Temkin isotherm, and Halsey isotherm was expressed by Equation (3), Equation (5), Equation (6), and Equation (7), respectively (Esmaili & Beni 2015):

$$\frac{1}{q_e} = \left(\frac{1}{K_L \cdot q_{\max}} \right) \frac{1}{C_e} + \frac{1}{q_{\max}} \quad (3)$$

where the quantity adsorbed and uranium concentration at the adsorption equilibrium of the strain are expressed as q_e (mg/g) and C_e (mg/L), respectively. q_{\max} (mg/g) is the theoretical maximum saturation adsorption of the Langmuir isotherm, and K_L (mg/L) is the balance constant of sorption. Significantly, the non-dimensional separating factor (R_L) is defined by the Langmuir isotherm and is represented by Equation (4) (Guo & Wang 2019):

$$R_L = \frac{1}{1 + K_L \cdot C_0} \quad (4)$$

where C_0 (mg/L) is the initial uranium concentration, and the K_L (mg/L) value is the equilibrium constant in the Langmuir isotherm. Furthermore, when $0 < R_L < 1$, it indicated that the biosorption properties were favorable (Esmaili & Beni 2015). Freundlich and Temkin isothermal models were determined by Equations (5) and (6), respectively (Ezzati 2020):

$$\ln q_e = \ln K_f + \frac{1}{n} \ln C_e \quad (5)$$

$$q_e = \frac{RT}{b} \ln K_t + \frac{RT}{b} \ln C_e \quad (6)$$

where K_f ((mg/g), (L/mg)^{1/n}) and K_t (g/L) are the adsorption equilibrium constants of the Freundlich and Langmuir isothermal models, respectively. n is a constant, indicating a better interaction between the adsorbent and the adsorbate when $1/n$ was 0–1. R is the molar gas constant ($R = 8.314$ J/mol · K), T (K) is the absolute temperature and b is the isothermal constant. The Halsey model is formulated using Equation (7) (Ezzati 2020):

$$\ln q_e = \left[\frac{1}{m} \ln K_h \right] - \frac{1}{m} \ln \left(\frac{1}{C_e} \right) \quad (7)$$

where K_h and $1/m$ are the equilibrium constants and exponents of the Halsey isothermal model.

The adsorption equilibrium model was used to fit the experimental data to calculate the linear correlation parameters of the model. As shown in Figure 5 and Table 1, the experimental data did not agree well with the Langmuir isotherm, with a correlation coefficient ($R^2 = 0.80$), whereas it showed a good agreement with Freundlich and Temkin isotherm models over a wide range of sorption concentrations ($R_f^2 = 0.97$, $R_t^2 = 0.96$). This indicated that the adsorption of U(VI) ions by the strain ZFSY-01 was consistent with the inhomogeneous surface multilayer sorption under non-ideal conditions. Significantly, the fitting results of the Halsey isothermal model were also excellent ($R_h^2 = 0.97$), and this model was also a multilayer adsorption model. The Freundlich isotherm model, $1/n = 0.29$ indicated that the strain was favorable to the adsorption of U(VI), and there was a strong interaction between sorbent and adsorbent.

3.4. Kinetic and thermodynamic analysis of uranium removal by strain ZFSY-01

Kinetic studies of biosorption are studied to better determine the adsorption mechanism of strain ZFSY-01 and control the chemical reaction rate. In this study, models of pseudo-first-order kinetic, pseudo-second-order kinetic as well as intraparticle diffusion have been used for fitting the test data. These linear equations of the model are represented by Equations (8)–(10), respectively (Wang *et al.* 2020):

$$\ln(q_e - q_t) = (\ln q_e - k_1 \cdot t) \quad (8)$$

$$\frac{t}{q_t} = \frac{1}{k_2 \cdot q_e^2} + \frac{1}{q_e} \cdot t \quad (9)$$

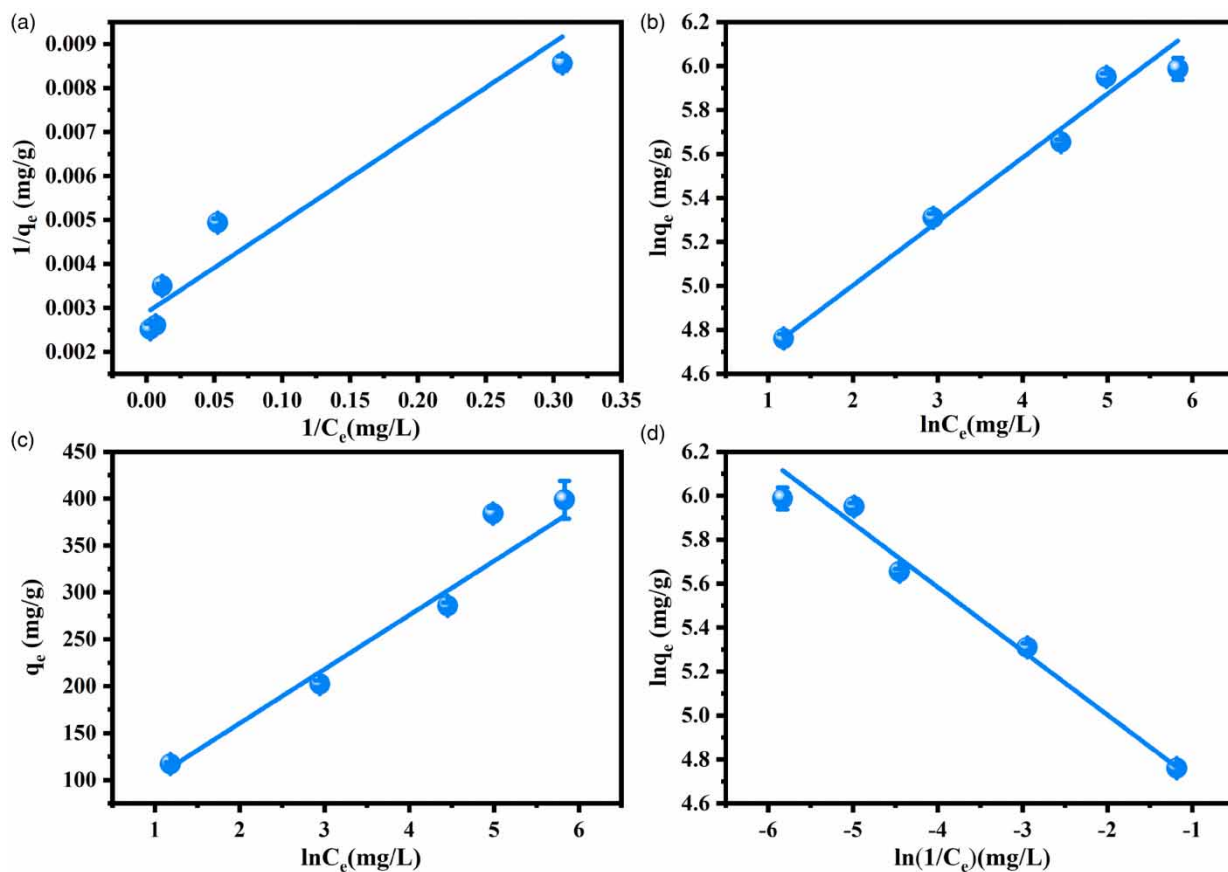


Figure 5 | Isotherm model for uranium adsorption by strain ZFSY-01. (a) Langmuir isotherm model. (b) Freundlich isotherm model. (c) Temkin isotherm model. (d) Halsey isotherm model (initial uranium concentration: 200 mg/L, T : 30 °C, strain dosage: 400 mg/L, reaction time: 4 h, pH: 6.5).

Table 1 | Isothermal model parameters for uranium adsorption by strain ZFSY-01

| Experimental value | Langmuir | | | Freundlich | | | Temkin | | | Halsey | | |
|--------------------|----------|-------------|---------|------------|-------|---------|--------|-------|---------|--------|--------------------|---------|
| | q_m | R_L | R_f^2 | K_F | $1/n$ | R_f^2 | RT/b | K_t | R_t^2 | $1/m$ | K_h | R_h^2 |
| 384.15 | 346.02 | 0.014–0.124 | 0.80 | 83.25 | 0.29 | 0.97 | 57.70 | 2.18 | 0.96 | 0.29 | 4.19×10^6 | 0.97 |

$$q_t = K_{in} \cdot t^{0.5} + C \quad (10)$$

The q_e (mg/g) and q_t (mg/g) are the adsorption capacity at the moment of t (min) and the moment of equilibrium in the adsorption process, respectively. K_1 (min^{-1}) is the pseudo-first-order kinetic adsorption rate constant and K_2 (g/mg·min) is the pseudo-second-order kinetic adsorption rate permanent. K_{in} (mg/g·min^{1/2}) is the model rate coefficient for intraparticle diffusion, and C (mg/g) is a constant in the boundary layer thickness function.

The fitting results of the experimental data are shown in Figure 6(a)–6(c) and Table 2. The regression coefficients ($R_1^2 = 0.79$, $R_2^2 = 0.99$) indicated that the experimental data are a good match for the pseudo-second-order kinetic model. Therefore, it was assumed that the process of uranium adsorption for this strain is mainly chemical adsorption. Meanwhile, the theoretical value $q_e = 301.2$ mg U/g was estimated by the pseudo-secondary model, which was basically consistent with the experimental value. Interestingly, in most previous studies, the pseudo-secondary kinetic model showed a good correlation with a fit coefficient $R^2 > 0.99$ (Tuzen *et al.* 2020). In addition, the intraparticle diffusion model also showed good agreement ($R_3^2 = 0.88$). Considering the complexity of the adsorption mechanism, this model is also employed to describe

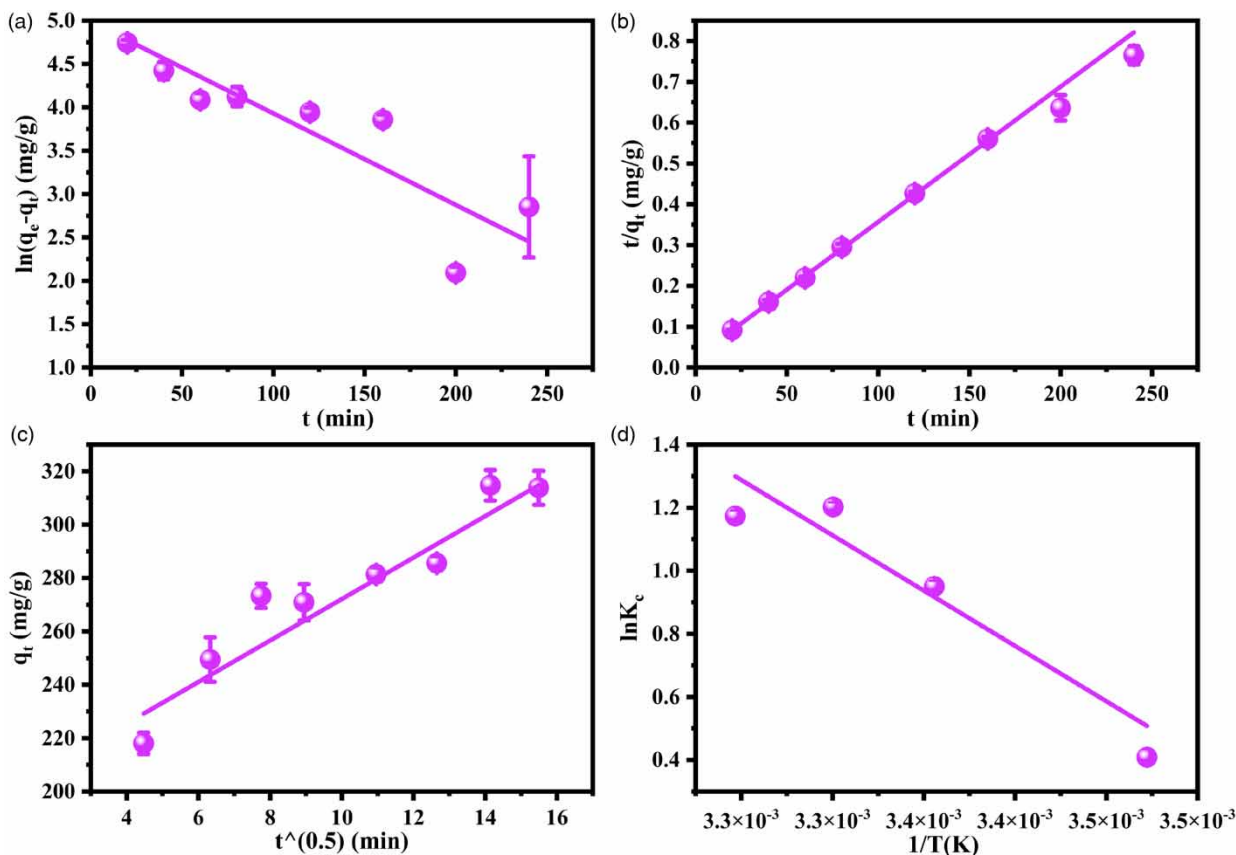


Figure 6 | Kinetic and thermodynamic models for the adsorption on uranium from strain ZFSY-01. (a) Pseudo-first-order kinetic model. (b) Pseudo-second-order kinetic model. (c) Intraparticle diffusion model (initial uranium concentration: 200 mg/L, strain dosage: 400 mg/L, T : 30 °C, pH: 6.5, V : 50 ml). (d) Thermodynamic parameter model (initial uranium concentration: 200 mg/L, V : 50 ml, T : 288, 298, 303, and 308 K, strain dosage: 400 mg/L, pH: 6.5).

Table 2 | Kinetic parameters of uranium adsorption by strain ZFSY-01

| Experimental value | Pseudo-first-order | | | Pseudo-second-order | | | Intraparticle diffusion | | |
|--------------------|--------------------|--------------|---------|---------------------|--------------|---------|-------------------------|---------|---------|
| | q_e (mg/g) | K_1 (/min) | R_1^2 | q_e (mg/g) | K_2 (/min) | R_2^2 | K_i | C | R_3^2 |
| 314.75 | 146.35 | 0.0243 | 0.79 | 301.20 | 0.00043 | 0.99 | 7.770 | 194.444 | 0.88 |

the mechanism of adsorption. To sum up, in the first stage, U(VI) was adsorbed by bacteria through the diffusion of pores inside and outside the membrane. Subsequently, U(VI) could be immobilized on the surface or inside of the bacteria through chemical reactions with organic functional groups on the surface of the bacteria.

To obtain more insight into the reaction process, the thermodynamic parameters of uranium adsorption by strain ZFSY-01 were investigated. At the temperature range of 288–308 K, the adsorption properties were studied by calculating (ΔG^0) (kJ/mol), (ΔH^0) (kJ/mol), and (ΔS^0) (J/mol·K). The relationships between the above three parameters are represented by the following equations (Smjecanin *et al.* 2022):

$$\Delta G^0 = \Delta H^0 - T\Delta S^0 \quad (11)$$

$$\ln K_c = \frac{\Delta S^0}{R} - \frac{\Delta H^0}{RT} \quad (12)$$

$$K_c = \frac{q_e}{C_e} \quad (13)$$

Table 3 | Thermodynamic characteristic parameters of uranium adsorption by strain ZFSY-01

| T (K) | ΔG^0 (kJ/mol) | ΔS^0 (J/(mol·K)) | ΔH^0 (kJ/mol) |
|---------|-----------------------|--------------------------|-----------------------|
| 288 | -1.21 | 105.51 | 29.17 |
| 298 | -2.27 | | |
| 303 | -2.79 | | |
| 308 | -3.32 | | |

where T (K) is the temperature, K_c and R are the balance constant as well as the constant of the gas, respectively. When $\Delta G^0 < 0$, it meant that the reaction could proceed spontaneously, and vice versa. The reaction was endothermic as $\Delta H^0 > 0$ and exothermic as $\Delta H^0 < 0$. If $|\Delta H^0| < 40$ kJ/mol, it meant that the system reaction was a physical process. Moreover, if $\Delta S^0 > 0$, it suggested an increase in the disorder of the adsorption system (Sahmoune 2019).

The thermodynamic parameters obtained from the experiments are shown in Table 3 and Figure 6(d). The enthalpy change ($\Delta H^0 = 29.17$ kJ/mol) demonstrated that the reaction process was physical and endothermic. Also, the entropy change ($\Delta S^0 = 105.51$ J/mol·K) as well as Gibbs free energy (-3.32 kJ/mol $< \Delta G^0 < -1.21$ kJ/mol) suggested that the U(VI) absorption by strain ZFSY-01 was an entropy-increasing process that could proceed spontaneously.

4. CONCLUSION

This research examined the bioabsorption of U(VI) by *J. quinghaiensis* strain ZFSY-01, which was isolated from the effluent of a uranium mine in northwest China. According to the aforementioned investigations, this strain was found to be highly tolerant to uranium, maintaining high cellular activity even at uranium concentrations of 300 mg/L and resulting in an adsorption capacity and efficiency of 391.5 mg U/g and 78.3%, respectively, under the ideal adsorption circumstances (initial uranium concentration: 200 mg/L, pH: 5, reaction time: 4 h, strain dosage: 400 mg/L, T : 30 °C). Significantly, it exhibited better adsorption properties compared to other biosorbent materials, especially since the adsorption capacity of this strain reached the maximum ($Q = 788.9$ mg U/g) under 100 mg/L of strain dosage. The obtained data were consistent with the Freundlich isothermal adsorption model, the Temkin isothermal adsorption model, the Halsey isothermal adsorption model, and the pseudo-second-order kinetic model with regression coefficients $R^2 > 0.95$ or more. Meanwhile, thermodynamic parameters indicate that the adsorption of U(VI) by strain ZFSY-01 is a spontaneous endothermic process. As a result, it was postulated that the mechanism for U(VI) immobilization by this strain involved a combination of chemical and physical adsorption. Based on the above results, the strain ZFSY-01 can effectively remove U(VI) ions from high- or low-concentration uranium-containing wastewater and is a promising biosorbent. However, further research is needed to achieve industrial application.

ACKNOWLEDGEMENTS

This work was supported by the National Natural Science Foundation of China (No. 32060292). In addition, the authors would like to thank the anonymous reviewers for their valuable comments.

DATA AVAILABILITY STATEMENT

All relevant data are included in the paper or its Supplementary Information.

CONFLICT OF INTEREST

The authors declare there is no conflict.

REFERENCES

- Banala, U. K., Das, N., Padhi, R. K. & Toleti, S. R. 2021a Alkaliphilic bacteria retrieved from uranium mining effluent: characterization, u sequestration and remediation potential. *Environmental Technology & Innovation* **24**, 101893.
- Banala, U. K., Indradyumna Das, N. P. & Toleti, S. R. 2021b Uranium sequestration abilities of *Bacillus* bacterium isolated from an alkaline mining region. *Journal of Hazardous Materials* **411**, 125053.

- Banerjee, S., Kundu, A. & Dhak, P. 2022 Bioremediation of uranium from waste effluents using novel biosorbents: a review. *Journal of Radioanalytical and Nuclear Chemistry* **331**, 2409–2435.
- Beni, A. A. & Esmaili, A. 2020 Biosorption, an efficient method for removing heavy metals from industrial effluents: a review. *Environmental Technology & Innovation* **17**, 100503.
- Ding, C., Wencai, C., Yubing, S. & Xiangke, W. 2014 Retraction: determination of chemical affinity of graphene oxide nanosheets with radionuclides investigated by macroscopic, spectroscopic and modeling techniques. *Dalton Transactions* **49**, 3888–3896.
- Esmaili, A. & Beni, A. A. 2015 Biosorption of nickel and cobalt from plant effluent by *Sargassum glaucescens* nanoparticles at new membrane reactor. *International Journal of Environmental Science and Technology* **12**, 2055–2064.
- Ezzati, R. 2020 Derivation of pseudo-first-order, pseudo-second-order and modified pseudo-first-order rate equations from Langmuir and Freundlich isotherms for adsorption. *Chemical Engineering Journal* **392**, 123705.
- Guo, X. & Wang, J. 2019 Comparison of linearization methods for modeling the Langmuir adsorption isotherm. *Journal of Molecular Liquids* **296**, 111850.
- Gupta, N. K., Sengupta, A., Gupta, A., Sonawane, J. R. & Sahoo, H. 2018 Biosorption – an alternative method for nuclear waste management: a critical review. *Journal of Environmental Chemical Engineering* **6**, 101893.
- Hu, W., Li, M., Chen, T., Zhang, Z., Chen, D. & Liu, H. 2018 Enrichment of U(VI) on *Bacillus subtilis*/Fe₃O₄ nanocomposite. *Journal of Molecular Liquids* **258**, 244–252.
- Islam, E. & Sar, P. 2011 Culture-dependent and -independent molecular analysis of the bacterial community within uranium ore. *Journal of Basic Microbiology* **51**, 372–384.
- Lakaniemi, A. M., Douglas, G. B. & Kaksonen, A. H. 2019 Engineering and kinetic aspects of bacterial uranium reduction for the remediation of uranium contaminated environments. *Journal of Hazardous Materials* **371**, 198–212.
- Li, X., Ding, C., Liao, J., Lan, T., Li, F., Zhang, D., Yang, J., Yang, Y., Luo, S., Tang, J. & Liu, N. 2014 Biosorption of uranium on *Bacillus* sp. dwc-2: preliminary investigation on mechanism. *Journal of Environmental Radioactivity* **135**, 6–12.
- Li, R., Ibeanusi, V., Hoyle, J., Crandall, C., Jagoe, C., Seaman, J., Anandhi, A. & Chen, G. 2019 Bacterial-facilitated uranium transport in the presence of phytate at savannah river site. *Chemosphere* **223**, 351–357.
- Liu, L., Jing, X., Dai, C., Zhang, Z. & Song, W. 2019 Kinetic and equilibrium of U(VI) biosorption onto the resistant bacterium *Bacillus amyloliquefaciens*. *Journal of Environmental Radioactivity* **203**, 117–124.
- Liu, L., Chen, J., Liu, F., Song, W. & Sun, Y. 2021 Bioaccumulation of uranium by *Candida utilis*: investigated by water chemistry and biological effects. *Environmental Research* **194**, 110691.
- Malekzadeh, F., Latifi, A. M., Shahamat, M., Levin, M. & Colwell, R. R. 2002 Effects of selected physical and chemical parameters on uranium uptake by the bacterium *Chryseomonas* MGF-48. *World Journal of Microbiology and Biotechnology* **18**, 599–602.
- Malkoc, E. & Nuhoglu, Y. 2005 Investigations of nickel (II) removal from aqueous solutions using tea factory waste. *Journal of Hazardous Materials* **127**, 120–128.
- Maolin, W., Shijun, W., Jianan, G., Zisheng, L., Yongqiang, Y., Fanrong, C. & Runliang, Z. 2022 Enhanced immobilization of uranium(VI) during the conversion of microbially induced calcite to hydroxylapatite. *Journal of Hazardous Materials* **434**, 128936.
- Nie, X., Yiqian, W., Faqin, D., Wencai, C., Xiaojing, L., Congcong, D., Qiaoya, L., Mingxue, L., Junling, W., Haichao, Z., Guozheng, C., Yan, Z. & Xiaolan, L. 2022 Surface interaction and biomineralization of uranium induced by the living and dead bacterial ghosts of *Kocuria* sp. *Journal of Environmental Chemical Engineering* **10**, 2–3.
- Özdemir, S. & Kilinc, E. 2012 *Geobacillus thermoleovorans* immobilized on Amberlite XAD-4 resin as a biosorbent for solid phase extraction of uranium (VI) prior to its spectrophotometric determination. *Microchimica Acta* **178**, 389–397.
- Pan, X. H., Chen, Z., Chen, F. B., Cheng, Y. J., Lin, Z. & Guan, X. 2015 The mechanism of uranium transformation from U(VI) into nano-uramphite by two indigenous *Bacillus thuringiensis* strains. *Journal of Hazardous Materials* **297**, 313–319.
- Pudza, M. Y. & Abidin, Z. Z. 2020 A sustainable and eco-friendly technique for dye adsorption from aqueous media using waste from *Jatropha curcas* (isotherm and kinetic model). *Desalination and Water Treatment* **182**, 365–374.
- Sahmoune, M. N. 2019 Evaluation of thermodynamic parameters for adsorption of heavy metals by green adsorbents. *Environmental Chemistry Letters* **17**, 697–704.
- Salome, K. R., Beazley, M. J., Webb, S. M., Sobecky, P. A. & TAILLEFERT, M. 2017 Biomineralization of U(VI) phosphate promoted by microbially-mediated phytate hydrolysis in contaminated soils. *Geochimica et Cosmochimica Acta* **197**, 27–42.
- Sánchez-Castro, I., Martínez-Rodríguez, P., Jroundi, F., Solari, P. L., Descostes, M. & Merroun, M. L. 2020 High-efficient microbial immobilization of solved U(VI) by the *Stenotrophomonas* strain Br8. *Water Research* **183**, 116110.
- Silas, K., Musa, Y. & Habiba, M. 2022 Effective application of *Jatropha curcas* husk activated ZnCl₂ for adsorption of methylene blue: isotherm, kinetics and development of empirical model. *Chemical Review and Letters* **5**, 153–160.
- Sivashankar, R., Sathya, A. B., Kanimozhi, J. & Deepanraj, B. 2022 Characterization of the biosorption process. In *Biosorption for Wastewater Contaminants* (Selvasembian, R. & Singh, P., eds.). John Wiley & Sons, New York, pp. 102–116.
- Smjecanin, N., Buzo, D., Masic, E., Nuhanovic, M., Sulejmanovic, J., Azhar, O. & Sher, F. 2022 Algae based green biocomposites for uranium removal from wastewater: kinetic, equilibrium and thermodynamic studies. *Materials Chemistry and Physics* **283**, 4–9.
- Song, J., Han, B., Song, H., Yang, J., Zhang, L., Ning, P. & Lin, Z. 2019 Nonreductive biomineralization of uranium by *Bacillus subtilis* ATCC-6633 under aerobic conditions. *Journal of Environmental Radioactivity* **24**, 208–209.

- Sourav, P., Prathap, S., Kumar, S. J., Debasish, P., Kumar, S. S., Kumar, S. S., Rok, L. Y., Syam, S. L. & Srinivas, R. K. 2022 Adsorptive sequestration of noxious uranium (VI) from water resources: a comprehensive review. *Chemosphere* **308**, 136278.
- Tong, K. 2017 Preparation and biosorption evaluation of *Bacillus subtilis*/alginate-chitosan microcapsule. *Nanotechnology Science and Applications* **10**, 35–43.
- Tsuruta, T. 2004 Adsorption of uranium from acidic solution by microbes and effect of thorium on uranium adsorption by *Streptomyces levoris*. *Journal of Bioscience and Bioengineering* **97**, 275–277.
- Tuzen, M., Saleh, T. A., Sar, A. & Naeemullah 2020 Interfacial polymerization of trimesoyl chloride with melamine and palygorskite for efficient uranium ions ultra-removal. *Chemical Engineering Research and Design* **159**, 353–361.
- Wang, J., Hu, X., Liu, Y., Xie, S. & Bao, Z. 2010 Biosorption of uranium (VI) by immobilized *Aspergillus fumigatus* beads. *Journal of Environmental Radioactivity* **101**, 504–508.
- Wang, Y., Nie, X., Cheng, W., Dong, F. & Marwani, H. M. 2018 A synergistic biosorption and biomineralization strategy for *Kocuria* sp. to immobilizing U(VI) from aqueous solution. *Journal of Molecular Liquids* **275**, 215–220.
- Wang, Y., Peng, C., Padilla-Ortega, E., Robledo-Cabrera, A. & López-Valdivieso, A. 2020 Cr(VI) adsorption on activated carbon: mechanisms, modeling and limitations in water treatment. *Journal of Environmental Chemical Engineering* **8**, 104031.
- Yu, H., Pang, J., Ai, T. & Liu, L. 2016 Biosorption of Cu^{2+} , Co^{2+} and Ni^{2+} from aqueous solution by modified corn silk: equilibrium, kinetics, and thermodynamic studies. *Journal of Taiwan Insyutet Chemical Engineeres* **62**, 21–30.
- Yu, S., Hongwei, P., Shuyi, H., Hao, T., Shuqin, W., Muqing, Q., Zhongshan, C., Hui, Y., Gang, S., Dong, F., Baowei, H. & Xiangxue, W. 2021 Recent advances in metal-organic framework membranes for water treatment: a review. *Science of the Total Environment* **800**, 149662.
- Yu, Q., Yuan, Y., Feng, L., Sun, W., Lin, K., Zhang, J., Zhang, Y., Wang, H., Wang, N. & Peng, Q. 2022 Highly efficient immobilization of environmental uranium contamination with *Pseudomonas stutzeri* by biosorption, biomineralization, and bioreduction. *Journal of Hazardous Materials* **424**, 127758.

First received 31 March 2023; accepted in revised form 30 June 2023. Available online 12 July 2023